SUPPLEMENTARY DATA

Conducting-polymer nanocomposites as synergistic supports that accelerate electrocatalysis: PEDOT / nano Co_3O_4 / rGO as a photo catalyst of oxygen production from water

Mohammed Alsultan [a,b,*], Anwer M. Ameen [b], Amar Alkeisy [c], Gerhard F. Swiegers [a,d,*]

[a] *Intelligent Polymer Research Institute, University of Wollongong, Wollongong, NSW 2522, Australia*

[b] *Department of Science, College of Basic Education, University of Mosul, Mosul, 41002, Iraq*

[c] *Nanotechnology and Advanced Materials Research Center, University of Technology, Baghdad, 10066, Iraq*

[d] *ARC Centre of Excellence for Electromaterials Science, University of Wollongong, Wollongong, NSW 2522, Australia*

Gas analysis studies

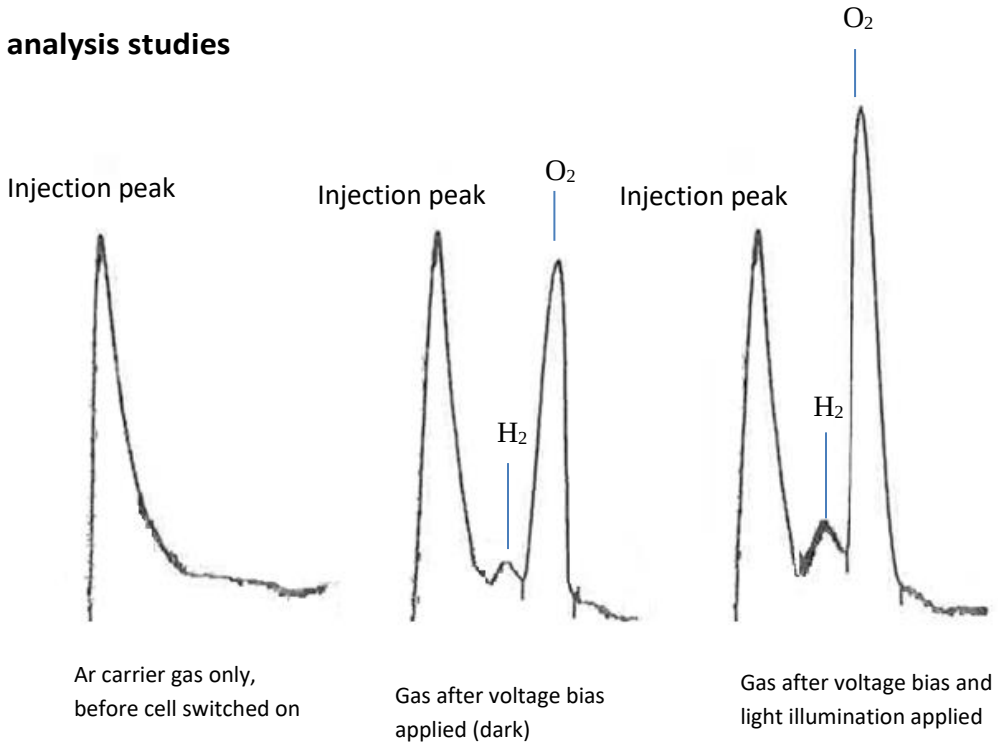

Fig. S1. Gas chromatography traces of gases collected from PEDOT / nano Co_3O_4 / rGO on FTO electrode.

The Faradaic efficiency for oxygen production was 61.2-62.1%, which means that this percentage of the electrons travelling through the circuit were converted into oxygen gas, which we physically collected in our apparatus. This is the conventional way of reporting gas production in photocatalytic systems, where the quantity of electrons passing through the cell is more accurately determined than the absolute weight of catalyst. For the record, that equates to 1.3 mmol/min in the dark and 1.7 mmol/min in the light, which figures could have been calculated from the Faradaic efficiency

Powder x-ray monitoring of the reduction of GO to rGO

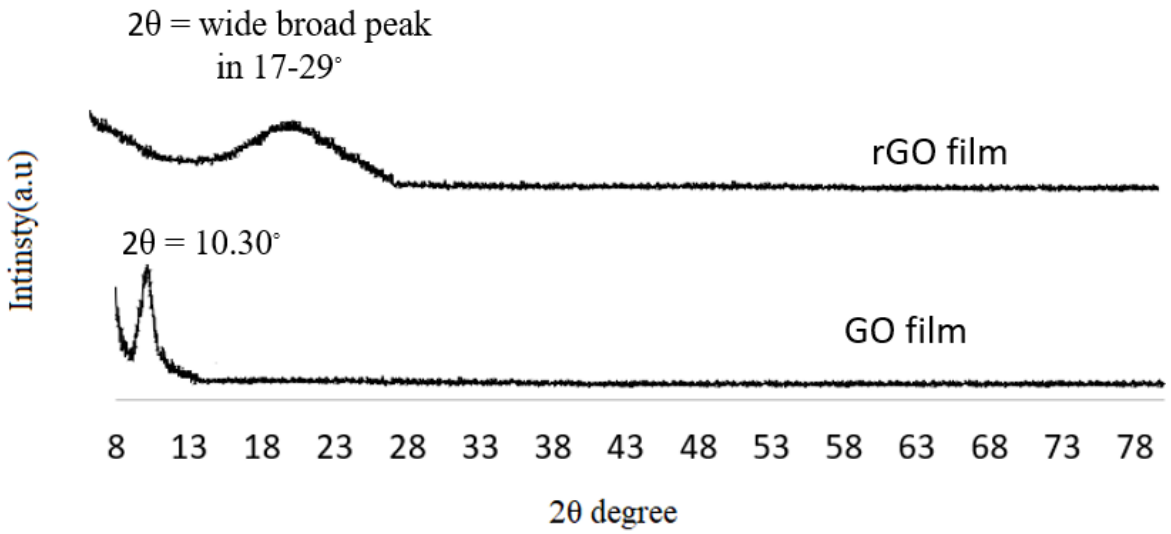

Fig. S2. XRD of GO and rGO film

As can be seen in Fig. S2, the GO[3-5] initially present was totally removed after scanning the film in cyclic voltammetry, while a broad peak appearing in the range 2θ = 18.28°-26.8° confirms the presence of rGO.[6]

Electrochemical impedance spectroscopy (EIS) and Tafel plot studies

Fig.7(b)-(c) shows Nyquist plots. A large arc observed in the main plots is attributed to intermediate to low frequencies (10-100 Hz) while another small arc is at high frequencies (1,000-10,000 Hz). The small arc characterizes the charge transfer during catalytic OER. Previous studies confirmed that at pH 12, adsorption processes dominate, such as ionic transfer (charge carriers) from diffuse layer to the catalyst itself.[1]

The Nyquist plots were modelled with the equivalent circuit shown in Fig.7 (a). Table 1 shows the results of the modelling. A qualitative measure of the electrochemically active surface area of the samples is provided by the capacitance C_{dl}. As can be seen, the most active Pt/PEDOT/nano-Co_3O_4/rGO film in both dark and light states exhibits a substantially lower capacitance C_{dl} than the Pt only control film. The resistivity of the most active PEDOT/nano-Co_3O_4/rGO on Pt / FTO, which is dependent on both the adsorption process (R_{ad}), and the charge transfer resistance, R_{CT}, is lower (in R_{ad} and R_{CT} values) than the resistivity of the bare Pt control; this made it more active per unit area under the testing conditions. This may be due, in part, to the formation of an oxide layer, which is known to form on Pt in basic solution.[2] The catalyst activity further increased when the light was switched off. The PEDOT control film displayed a smaller area resulting in lower catalytic activity.

Fig. 7(d) depicts Tafel plots of the various catalytic films. Data from these studies are recorded in the last two columns of Table 1. The exchange current density, i_o, presents the measured catalysis rate at reversible potential, when the overpotential is equal to zero. As can be seen in Table 1, the bare Pt control displayed the highest i_o, as may be expected. This indicated that it had the highest intrinsic catalytic capability at zero overpotential. Interestingly, PEDOT/nano-Co_3O_4/rGO on Pt / FTO film produced lower Tafel plots than the control films in both dark and under illumination. Under external bias the catalytic

OER activity of the Pt/PEDOT/nano-Co_3O_4/rGO required only 97.4 mV (without light illumination) and 93.7 mV (with light illumination) to increase the reaction rate by a factor of more than 8. The bare Pt control required 250 mV. It seems possible that the external applied bias improved reactant adsorption on the film surface, especially under light illumination.

X-ray photoelectron spectroscopy (XPS) studies

The PEDOT/nano-Co_3O_4/rGO film was further analysed using X-ray photoelectron spectroscopy (XPS) (Fig. S3). The main peaks in the data are attributed to S 2p, O 1s, C 1s, Co 2p and O 1s. Both O 1s and C 1s spectra can refer to PEDOT and rGO, while the S 2s spectrum derived only from the PEDOT. The C 1s spectrum contained six deconvolution peaks at 284.0, 284.80, 286.20, 286.78, 287.88, 289 and 291.03 eV (Fig. S3(b)). The peak at 284.0 eV represented a sp^2 carbon hybrid, which mainly related to the C=C binding energy.[5-6] The peak at 284.90 eV represented a sp^3 carbon hybrid and related to C-C, C-H while the peaks at 286.20, 286.78, 287.88, 289.21 and 291.03 eV corresponded to C-S, C-O, C=O, O-C=O and π-π interaction respectively.[5-6] The S 2p XPS spectrum of the film contained peaks at 163.5 and 165.5 eV, which relate to the binding energy of the $2p_{3/2}$ and $2p_{½}$ that correspond to the C-S bond and S^+.[5-6] These are assigned to the S atoms of the PEDOT fragments. The other two small peaks relate to the $2p_{3/2}$ and $2p_{½}$ of the sulfonic groups in the PTS structure.[5-6] The O 1s XPS spectra of the film displayed four peaks at 529.9, 530.3, 532 and 533 eV. The first two peaks that at 529.9 and 530.3 eV related to the existence of Co-O bonds, as is consistent with the Co 2p spectrum[5-6] for more detail the peak sites at 529.9 eV corresponding to lattice O, and the peak at 530.3 eV can be attributed to the low coordinated oxygen ions (chemisorbed oxygen) at the surface. The other two peaks that sited at 532 and 533 eV referring to the binding energy of C=O and C-O bonds respectively. [5-6] Finally, for the Co 2p spectra there were mainly two of binding energies observed at of 780 and 795.1 eV that assigned to the tetrahedral Co^{2+} and octahedral Co^{3+} contributed to the spin-orbit doublet 2p spectral profile of Co_3O_4. These peaks correspond to $2p_{1/2}$ and $2p_{3/2}$ with energy separation of 15.1 eV, as well as there were weak satellite structure found in the high binding energy side of $2p_{3/2}$ and $2p_{1/2}$ transitions referred to the co-existence of Co(II) and Co(III) on the material surface. [5-6]

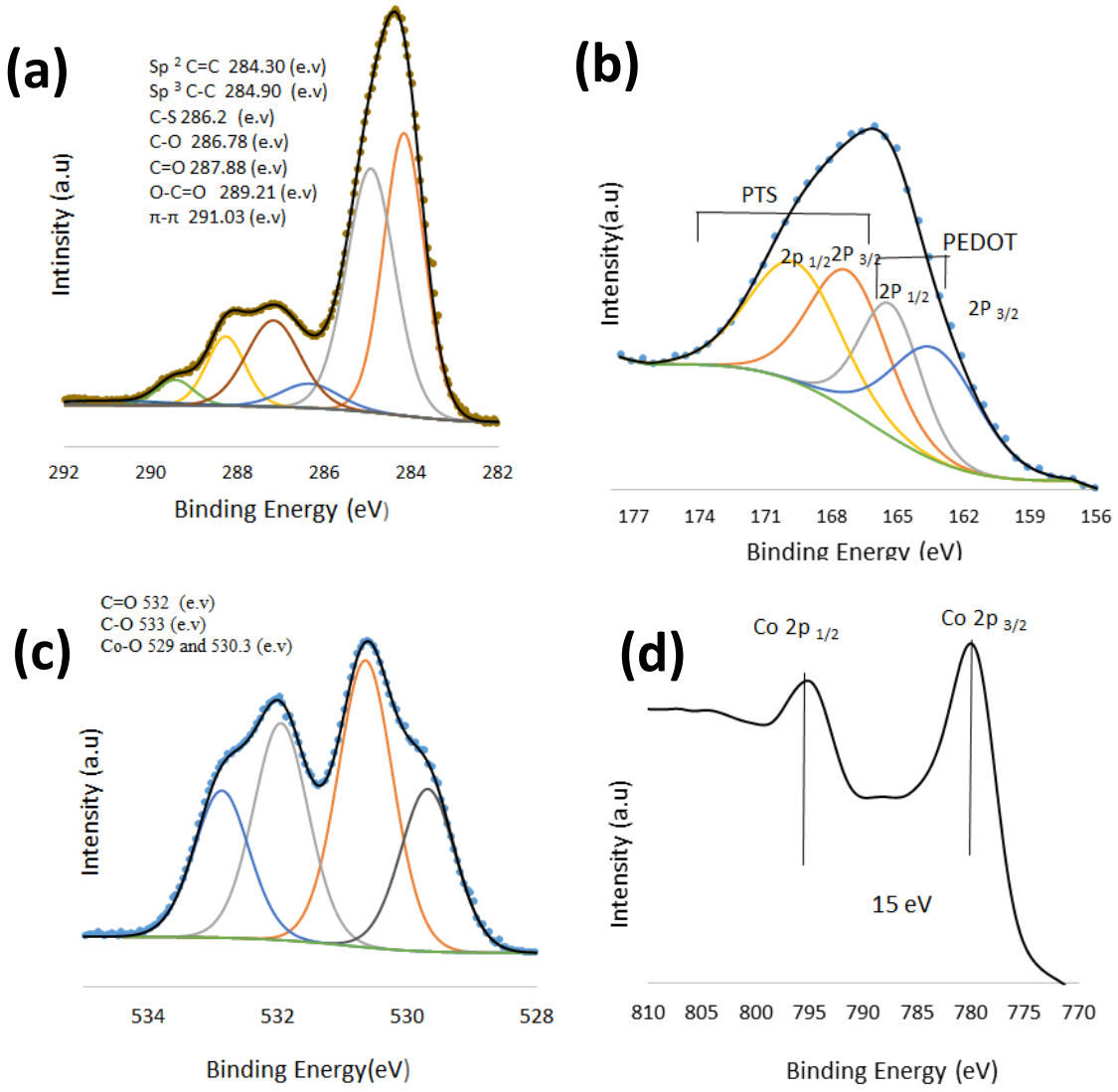

Fig. S3. XPS spectra of PEDOT/nano-Co_3O_4/rGO showing various binding energy regions; peaks representing the depicted transitions are shown, along with simulations (solid lines) and measured data (individual points). C 1s spectra and O 1s derive from both PEDOT and rGO while S 2p derives from PEDOT only and Co 2p derives from nano-Co_3O_4

UV-Vis absorption

The UV-Vis absorption spectra in Fig. S4 show that rGO, PEDOT and PEDOT/Co_3O_4/rGO absorb light in the wavelength range 500-800 nm.

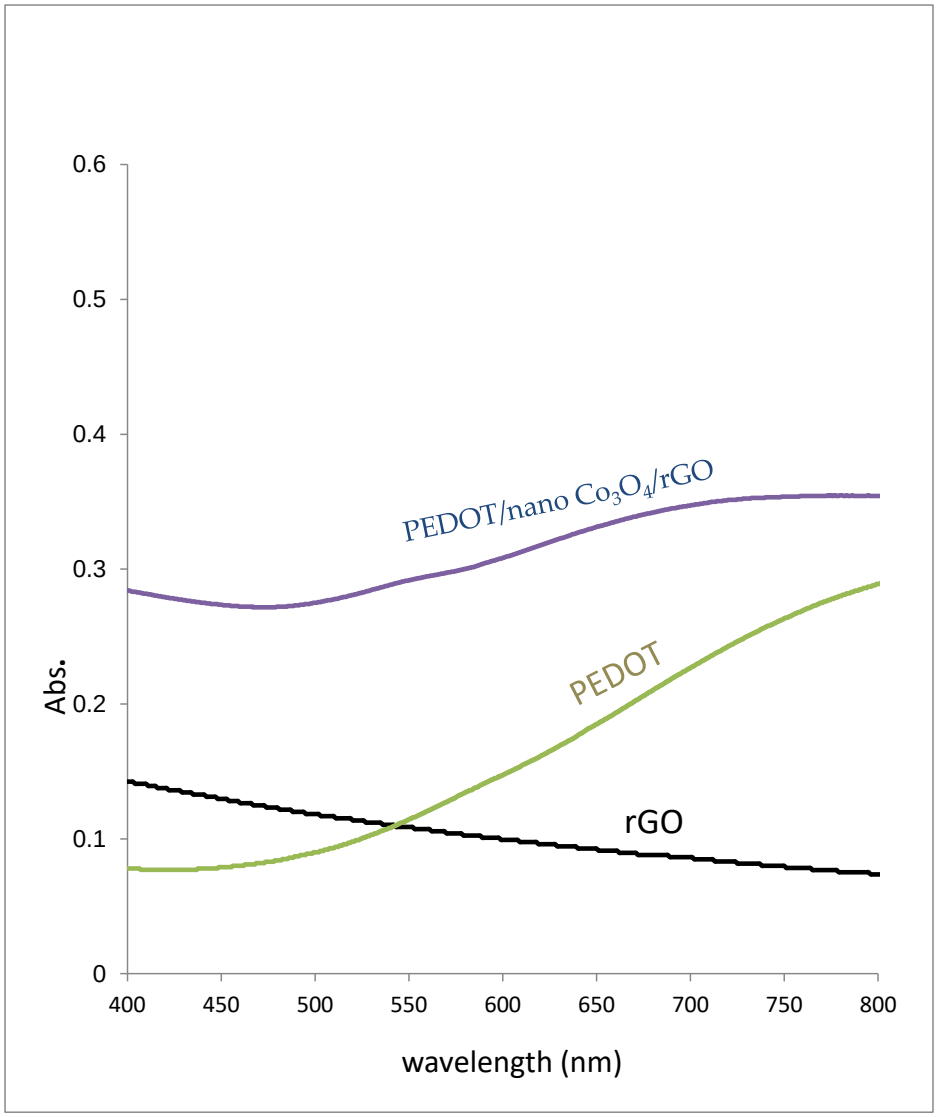

Fig. S4. UV-Vis spectra of rGO, PEDOT, and PEDOT/nano-Co_3O_4/rGO.

Additional references

1. Shimizu, K.; Lasia, A.; Boily, J.-F., Electrochemical Impedance Study of the Hematite/Water Interface. *Langmuir* **2012,** *28* (20), 7914-7920.
2. Corrigan, D. S.; Krauskopf, E. K.; Rice, L. M.; Wieckowski, A.; Weaver, M. J., Adsorption of acetic acid at platinum and gold electrodes: a combined infrared spectroscopic and radiotracer study. *The Journal of Physical Chemistry* **1988,** *92* (6), 1596-1601.
3. Liu, X.; Huang, J.; Wei, X.; Yuan, C.; Liu, T.; Cao, D.; Yin, J.; Wang, G., Preparation and electrochemical performances of nanostructured CoxNi1−x(OH)2 composites for supercapacitors. *Journal of Power Sources* **2013,** *240*, 338-343.
4. Zhao, Y.; He, S.; Wei, M.; Evans, D. G.; Duan, X., Hierarchical films of layered double hydroxides by using a sol–gel process and their high adaptability in water treatment. *Chemical Communications* **2010,** *46* (17), 3031-3033.
5. Alsultan, M.; Balakrishnan, S.; Choi, J.; Jalili, R.; Tiwari, P.; Wagner, P.; Swiegers, G. F., Synergistic Amplification of Water Oxidation Catalysis on Pt by a Thin-Film Conducting Polymer Composite. *ACS Applied Energy Materials* **2018,** *1* (8), 4235-4246, and references therein.
6. Alsultan, M.; Choi, J.; Jalili, R.; Wagner, P.; Swiegers, G. F., Synergistic amplification of catalytic hydrogen generation by a thin-film conducting polymer composite. *Catalysis Science & Technology* **2018,** *8* (16), 4169-4179, and references therein.